مجلة جامعة فزان العلمية
Fezzan University scientific Journal
journal@fezzanu.edu.ly

A Cost-Efficient Dual-Stage MPPT Solar Charge Controller with IoT Integration for Reliable Energy Storage in Power-Deficient Regions

*Hala N. Abu Mezyed[1] and Hala J. El-Khozondar[1,2]
[1]Electrical Engineering and Smart Systems Departments, Islamic University of Gaza,
[2]Materials, Engineering Faculty, Imperial, UK

Abstract
This paper presents the design, simulation, and evaluation of a cost-efficient, dual-stage Maximum Power Point Tracking (MPPT) solar-charge controller integrated with an Internet of Things (IoT) monitoring system, aimed at enhancing reliable energy storage in regions characterized by frequent power interruptions, such as the Gaza Strip. The proposed system adopts a cascaded DC–DC converter architecture, in which a Ćuk converter performs high-efficiency Maximum Power Point Tracking (MPPT) using the Perturb and Observe (P&O) algorithm, while a subsequent Buck converter provides stable and safe charging of a 12 V lead-acid battery. This dual-stage configuration effectively decouples the process of power extraction from voltage regulation, thereby optimizing overall system performance. The controller was rigorously evaluated through MATLAB/Simulink simulations using a user-defined photovoltaic (PV) array. The obtained results demonstrate robust and rapid dynamic tracking performance, with convergence times ranging between 0.048 s and 0.165 s under varying environmental conditions. The Perturb and Observe (P&O) algorithm successfully extracted maximum power, achieving 265 W under standard test conditions (1000 W/m², 25 °C) and 132 W under reduced irradiance conditions (500 W/m², 25 °C). Furthermore, real-time monitoring was implemented using an ESP32 microcontroller connected to the Arduino IoT Cloud, enabling continuous visualization of critical system and meteorological parameters. The proposed approach provides a reliable, high-efficiency, and easily monitored solution, offering a practical pathway for improving energy utilization in small-scale off-grid photovoltaic (PV) systems.

Keywords: AI, MATLAB/Simulink, Ćuk converter, Buck converter, solar cell, MPPT

Introduction and Previous Studies

Driven by concerns about climate change and global warming, the global installed capacity of renewable energy increased by 50% in 2024. By the end of 2024, the total installed capacity of renewable energy sources—including solar, wind, hydropower, geothermal, marine, and biogas—reached approximately 4,448.1 GW, of which about 2,200 GW was attributed to photovoltaic (PV) systems. This rapid expansion reflects a global transition toward sustainable and renewable energy technologies [1,2].

* Research author: Email addresses Hala.mezyed@gmail.com– Seminar on the transition to clean energy in Fezzan: Renewable energy engineering in esert regions – Thursday, February 12, 2026

Solar photovoltaic (PV) energy has emerged as one of the most promising renewable energy sources for meeting the growing global electricity demand while reducing environmental pollution [3–9]. In addition to reducing dependence on fossil fuels, which are finite and subject to depletion, solar energy provides a sustainable long-term alternative.

Solar PV technology has been extensively studied in both standalone configurations [15–19] and hybrid energy systems [20–30]. Its attractiveness is further enhanced in regions with high solar irradiance, such as the Middle East, where it is particularly suitable for addressing persistent electricity shortages. For instance, the Gaza Strip experiences frequent power interruptions that significantly affect daily life [31–33]. In such contexts, PV systems offer a clean and sustainable solution for reducing reliance on conventional fossil-fuel-based generation.

However, the performance of PV modules is highly dependent on environmental conditions, including solar irradiance, temperature variations, and partial shading. These factors continuously affect the maximum power point (MPP) of the PV array [34,35]. Without effective tracking of the MPP, a significant portion of available solar energy cannot be extracted [36].

To overcome this limitation, extensive research has focused on the development of Maximum Power Point Tracking (MPPT) algorithms that enable PV systems to operate efficiently under dynamic conditions [37–42]. Conventional methods such as Perturb and Observe (P&O) and Incremental Conductance (INC) are widely used due to their simplicity and ease of implementation [43]. However, they suffer from limitations such as slow dynamic response and steady-state oscillations, particularly under rapidly changing irradiance conditions [22].

Recent studies from the Middle East have proposed improved MPPT techniques based on intelligent control and optimization methods. Kaaitan et al. [39] developed a global MPPT method using the Sooty Tern Optimization Algorithm (STOA), achieving a tracking efficiency of 99.94% under partial shading conditions. Similarly, Alkarasneh et al. [40] proposed a hybrid fuzzy-logic-based P&O controller that effectively handles sudden irradiance variations while reducing oscillations. In Lebanon and the United Arab Emirates, Osmani et al. [34] introduced a lithium-ion solar charger with an interleaved DC–DC converter and modified P&O algorithm, achieving efficiencies between 87% and 100%. Furthermore, Hadi [42] developed an adaptive variable-step P&O algorithm that significantly improved system dynamic performance. Collectively, these studies demonstrate growing regional progress in high-efficiency MPPT systems.

Despite these developments, many small-scale PV installations in the Middle East still rely on simple pulse-width modulation (PWM) charge controllers. Although cost-effective, these controllers cannot extract maximum power from PV systems, leading to reduced energy utilization and lower charging efficiency, particularly in standalone applications. Therefore, there is a strong need for low-cost, efficient MPPT-based solar charge controllers that ensure optimal power extraction and safe battery charging [43].

In this paper, a dual-stage MPPT solar charge controller is proposed. The system integrates a Ćuk converter with a Perturb and Observe (P&O) MPPT algorithm for maximum power extraction, followed by a Buck converter dedicated to charging a 12 V battery. The system is simulated using MATLAB/Simulink based on real PV data and incorporates an Internet of Things (IoT) monitoring platform for real-time tracking of voltage, current, and battery status [44,45].

The proposed system introduces a cost-efficient dual-stage DC–DC architecture that decouples power extraction from voltage regulation. The Ćuk converter is used for high-efficiency MPPT operation, while the Buck converter ensures stable battery charging. The system achieves fast and robust tracking under varying irradiance and temperature conditions, with convergence times as low as 0.048 s. In addition, the integration of an IoT-based monitoring system using an ESP32 microcontroller enables real-time visualization and analysis of electrical and environmental parameters, which is rarely implemented in small-scale off-grid PV systems. These features make the proposed approach suitable for reliable energy storage applications in regions with frequent power interruptions, such as the Gaza Strip.

The main objectives of this study are:

- Maximize PV Power Extraction: Design a dual-stage DC–DC system capable of efficiently tracking and harvesting maximum power using a Ćuk converter with the Perturb and Observe (P&O) MPPT algorithm under varying environmental conditions.
- Ensure Safe and Stable Battery Charging: Implement a Buck converter stage to regulate and stabilize the output voltage for reliable charging of a 12 V lead-acid battery, thereby decoupling power extraction from voltage regulation.
- Enable Real-Time Monitoring and Control: Develop an IoT-based system using an ESP32 microcontroller for continuous data acquisition, remote visualization, and performance analysis of electrical and environmental parameters.

Materials and Methods

Proposed Model

The proposed system is designed to improve the efficiency of solar energy conversion and storage through a dual-stage DC–DC architecture composed of a Ćuk converter and a Buck converter. The main objective is to maximize power extraction from a photovoltaic (PV) module under varying environmental conditions while ensuring safe and stable charging of a 12 V lead-acid battery.

In this configuration, the Ćuk converter functions as the primary Maximum Power Point Tracking (MPPT) stage, controlled by the Perturb and Observe (P&O) algorithm. This algorithm continuously adjusts the converter duty cycle to maintain operation of the PV array at its maximum power point. The Buck converter operates as a secondary stage, reducing and stabilizing the output voltage of the Ćuk converter to match the battery charging requirements.

Both converters are operated in continuous conduction mode (CCM) to minimize current ripple and switching losses, thereby enhancing overall system efficiency. MATLAB/Simulink simulations, based on a parameterized PV array (Vmp = 31 V, Imp = 8.55 A, Pmax = 265 W), demonstrate that the dual-stage architecture effectively decouples power extraction from voltage regulation. Specifically, the Ćuk converter maintains optimal PV operation, while the Buck converter ensures stable battery charging.

As shown in Figure 1, this topology is particularly effective when the PV panel voltage differs significantly from the required battery charging voltage. In addition, an Internet of Things (IoT)-based monitoring module using an ESP32 microcontroller is integrated to enable real-time acquisition and remote visualization of electrical and environmental parameters via the Arduino IoT Cloud. This framework provides a cost-effective, modular, and efficient solution

for small-scale solar energy systems in off-grid regions with unreliable grid access, such as the Gaza Strip.

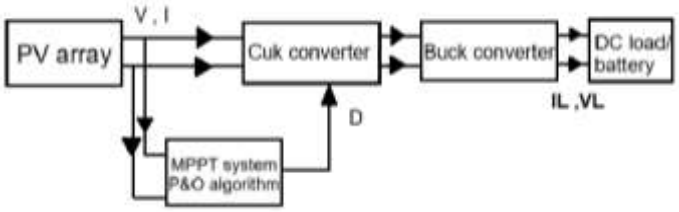

Figure 1: Block Diagram of Direct Duty Cycle Control MPPT

Figure 1 illustrates the block diagram of the proposed photovoltaic (PV) energy conversion system, including its main components and signal flow. The PV panel voltage and current are continuously measured and fed into the MPPT controller, which operates based on the Perturb and Observe (P&O) algorithm.

The controller dynamically adjusts the operating point of the PV system to ensure maximum power extraction. The resulting control signal generates a pulse-width modulation (PWM) waveform that drives the gate of the MOSFET in the Ćuk converter, regulating its switching operation.

In parallel, a Buck converter is used to step down the output voltage of the Ćuk converter to a suitable level for either DC load supply or battery charging. This dual-converter configuration enables efficient power conditioning and flexible energy management between storage and load requirements.

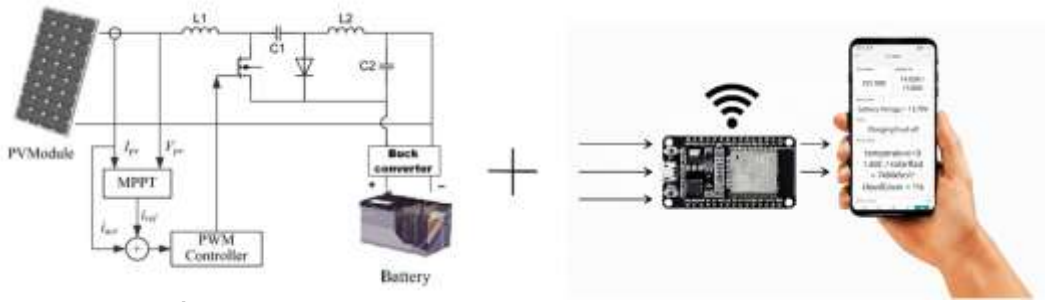

Figure 2: Ćuk and Buck Converters with IoT-Based MPPT Charge Controller

Figure 2 presents the circuit-level implementation of the Ćuk converter and the overall system architecture. The diagram identifies the input/output terminals and illustrates the PWM control interface connected to the Ćuk converter.

The Ćuk converter operates in coordination with the Buck converter, and both are connected to the battery storage system. In addition, an IoT platform is integrated into the system, enabling real-time monitoring of operational parameters through a cloud-based mobile application.

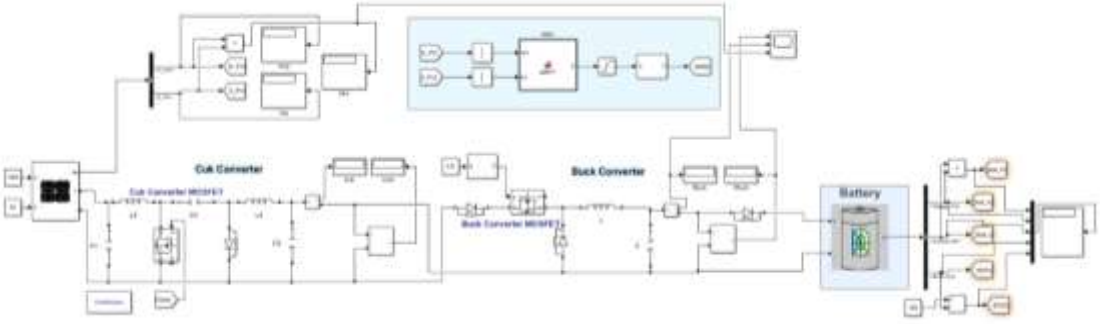

Figure 3: Simulated MPPT Model in MATLAB/Simulink

Figure 3 illustrates the operational structure of the proposed PV energy conversion system implemented in MATLAB/Simulink. The system consists of a PV array, an MPPT controller, and cascaded DC–DC converters.

The PV array produces variable DC output depending on solar irradiance and temperature. These parameters are continuously measured and supplied to the MPPT controller, which calculates the optimal duty cycle required to maintain operation at the maximum power point (MPP) by evaluating instantaneous power.

The resulting PWM signal is applied to the MOSFET gate of the Ćuk converter, ensuring regulation of the PV operating voltage near its optimal value. The Ćuk converter thus enables efficient energy extraction under dynamic environmental conditions.

The output of the Ćuk converter is subsequently processed by the Buck converter, which functions as a voltage regulation stage. This converter steps down the voltage to a stable level suitable for charging a 12 V lead-acid battery.

This cascaded structure separates the functions of power maximization and voltage regulation, allowing each converter to operate within its optimal performance range. Consequently, the system achieves improved dynamic response, reduced oscillations around the MPP, and stable battery charging under fluctuating irradiance and temperature conditions.

Methodology

PV Array Modeling and Characterization Using MATLAB/Simulink

The electrical behavior of the photovoltaic (PV) module was modeled using the PV Array block in the MATLAB/Simulink Electrical library, as shown in Figure 4. This block is based on the single-diode equivalent circuit model, which represents the fundamental physical processes of a silicon solar cell, including photogenerated current, diode saturation current, series resistance, and shunt resistance. The model enables accurate reproduction of the current–voltage (I–V) and power–voltage (P–V) characteristics under varying environmental conditions, such as solar irradiance and temperature [32,34–36].

The PV array was configured with one series-connected module and one parallel string. Electrical parameters—including short-circuit current (Isc), open-circuit voltage (Voc), maximum power point voltage (Vmp), maximum power point current (Imp), temperature coefficients, and cell configuration—were obtained from the manufacturer's datasheet (Appendix A). These parameters define the operating limits of the module and ensure that the simulation accurately represents real PV behavior.

Standard Test Conditions (STC) were initially applied, corresponding to a solar irradiance of 1000 W/m² and a cell temperature of 25 °C, in accordance with IEC 61215 standards [46]. Under these conditions, the PV Array block generated the I–V and P–V characteristics used directly in the MPPT and DC–DC converter simulations [36].

Effect of Solar Irradiance

To evaluate the impact of solar irradiance, the I–V characteristics were simulated at a constant temperature of 25 °C for different irradiance levels, as shown in Figure 5. A significant reduction in short-circuit current was observed with decreasing irradiance due to atmospheric variations such as cloud coverage, whereas the open-circuit voltage exhibited only minor changes.

This behavior is explained by the nearly linear dependence of photogenerated current on irradiance, while the open-circuit voltage varies logarithmically with light intensity [36].

The corresponding P–V curves, illustrated in Figure 6, show a proportional decrease in maximum output power with decreasing irradiance. Since output power is the product of voltage and current, the reduction in current directly limits the maximum achievable power at the MPP [37].

Effect of Temperature

The effect of temperature was analyzed by simulating the PV array under a constant irradiance of 1000 W/m² for different cell temperatures. As illustrated in Figure 7, the output current remained nearly constant, while the terminal voltage decreased significantly with increasing temperature.

This behavior is attributed to the increase in diode saturation current and enhanced carrier recombination at higher temperatures, which reduce the semiconductor bandgap and consequently decrease the open-circuit voltage [36].

Figure 8 presents the corresponding P–V characteristics under varying temperatures. The maximum power point shifts toward lower voltages as temperature increases, resulting in a reduction in maximum extractable power. This temperature-induced degradation is a well-established characteristic of silicon PV modules and has a direct impact on overall system efficiency [36].

Figure 1: PV block in Simulink

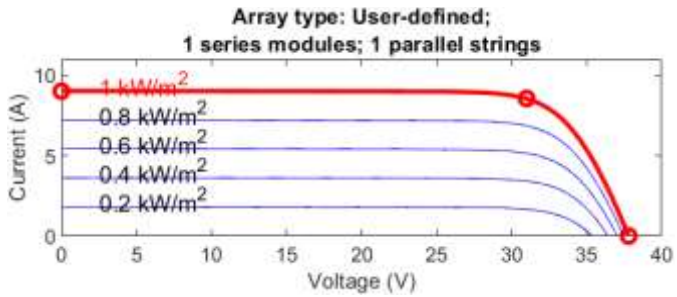

Figure 2. I-V curve for PV array generated on Simulink at 25 °C and different irradiances

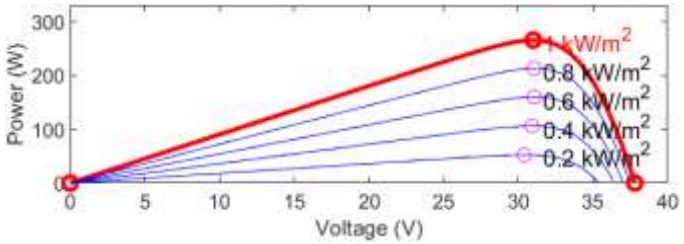

Figure 3. P-V curve for PV array generated on Simulink at 25 °C and different irradiances

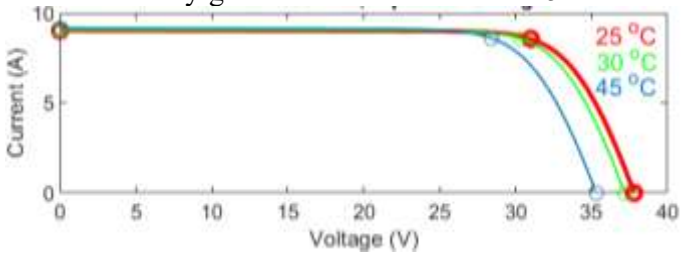

Figure 7. I-V curve for PV array generated on Simulink at 1000 W/m² and different temperatures

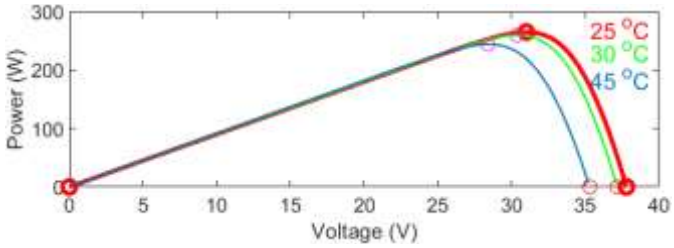

Figure 8. P–V curve for the PV array generated in Simulink at 1000 W/m² under different temperatures.

Ćuk Converter (MPPT Stage)

The Ćuk converter, illustrated in Figure 9, was designed to ensure efficient power transfer between the photovoltaic (PV) source and the load while enabling stable maximum power point tracking (MPPT). Since the primary objective of this stage is to regulate the PV voltage at its maximum power point (Vmp), the converter output voltage was selected to be approximately 30.5 V, closely matching the panel's nominal Vmp of 31 V.

The duty cycle of the Ćuk converter (DC) was determined based on the standard voltage conversion relationship [48]:

$$\frac{V_{out}}{V_{in}} = \frac{-D_C}{1 - D_C} \quad (1)$$

Selecting an output voltage close to Vmp improves the stability of the MPPT algorithm, as it enables the controller to converge more effectively toward the maximum power operating point. This approach reduces oscillations around the MPP and enhances the dynamic response of the system. Accordingly, a theoretical duty cycle of approximately 0.5 was obtained, while a practical value of DC = 0.49 was implemented. With Vin = 31 V and Vout ≈ 30.5 V, the converter operates efficiently within the desired voltage range.

A switching frequency of 30 kHz was selected to reduce current and voltage ripple while allowing the use of relatively small passive components. The inductors L1 = 0.6 mH and L2 = 0.583 mH, together with capacitors C1 = 0.237 mF and C2 = 12

μF, were designed to minimize ripple, ensure energy continuity, and maintain continuous conduction mode (CCM) under varying irradiance conditions.

Buck Converter (Battery Charging Stage)

The Buck converter, also shown in Figure 9, was designed to provide a regulated charging voltage of 13–14 V for a 12 V lead-acid battery. The duty ratio (DB) was selected to be approximately 0.6 to step down the Ćuk converter output voltage (~30 V) to the required charging level.

The voltage conversion relationship is given by [49]:

$$D_B = \frac{V_o}{V_{in}} \quad (2)$$

Based on this relationship, an output voltage of approximately 14 V was obtained. The inductor (L = 0.736 mH) and capacitor (C = 3 μF) were selected to ensure output voltage stability, reduce switching ripple, and maintain continuous conduction during battery charging.

Converter Performance with PV Array Input

Figure 9 presents the simulated Ćuk and Buck converter configurations using a PV array model as the input source. In the Ćuk converter stage, the PV panel voltage of 31 V (corresponding to Vmp) is regulated to approximately 29 V, which is close to the target operating point, with minimal ripple.

In the Buck converter stage, the regulated 29 V input is reduced to approximately 16.3 V, which is suitable for battery charging operation. The voltage and current waveforms, shown in Figure 10, exhibit acceptable ripple levels, confirming the stability and robustness of the proposed converter design under realistic PV operating conditions.

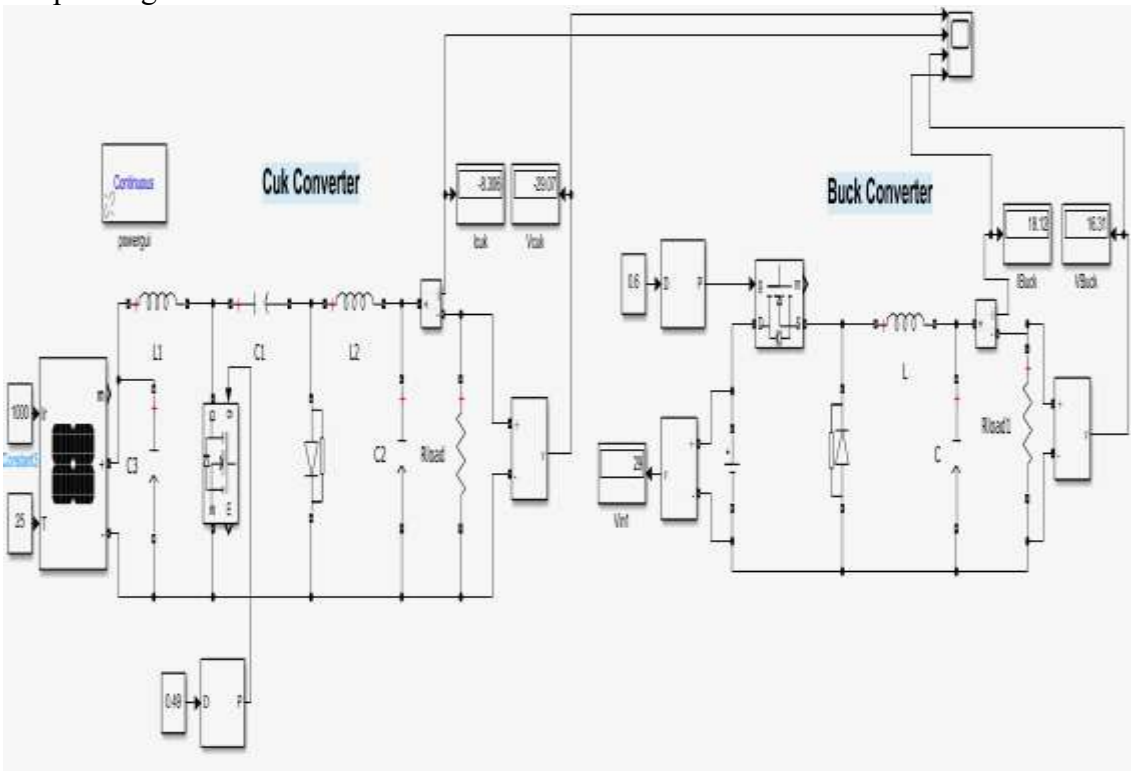

Figure 9. Simulink model of the tested Ćuk and Buck converters using a PV array as the input source.

Figure 10. Output voltages (V_{buck}, V_{cuk}) and currents (I_{buck}, I_{cuk}) as a function of time for the tested Ćuk and Buck converters with PV input

MPPT Algorithm — Perturb and Observe (P&O)

The Perturb and Observe (P&O) algorithm [50,51] was implemented to achieve maximum power point tracking (MPPT) in the photovoltaic (PV) system. The Simulink model of the MPPT controller is shown in Figure 11, while the operational logic is illustrated in Figure 12.

The P&O algorithm operates by periodically perturbing the PV operating voltage and observing the resulting change in output power. If the power increases following a perturbation, the operating point is adjusted in the same direction. If the power decreases, the perturbation direction is reversed. This iterative process guides the system toward the maximum power point (MPP) under varying irradiance and temperature conditions.

In the Simulink implementation, PV voltage and current are continuously measured to compute instantaneous power. The controller evaluates the incremental changes in power (ΔP) and voltage (ΔV), and updates the converter duty cycle accordingly.

A fixed duty-cycle step size of $\Delta D = 1 \times 10^{-5}$ was selected to achieve a balance between fast convergence and reduced steady-state oscillations around the MPP. The resulting PWM signal is used to drive the MOSFET (Metal-Oxide-Semiconductor Field-Effect Transistor) switch of the Ćuk converter, ensuring continuous operation near the optimal power point and maximizing energy extraction.

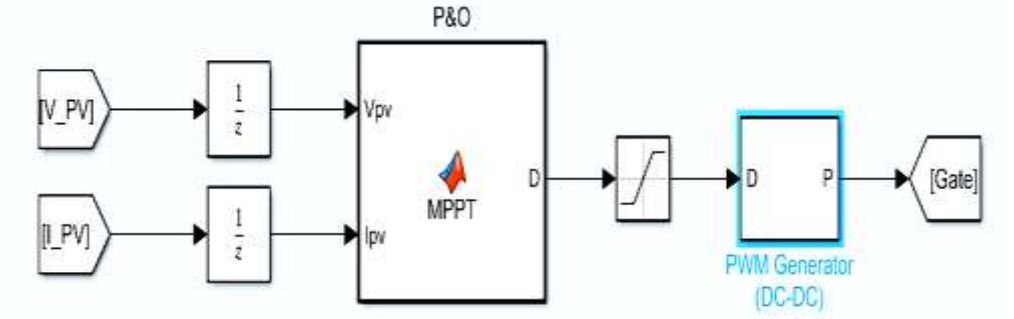

Figure 11. P&O MPPT and PWM Generator blocks in Simulink

k

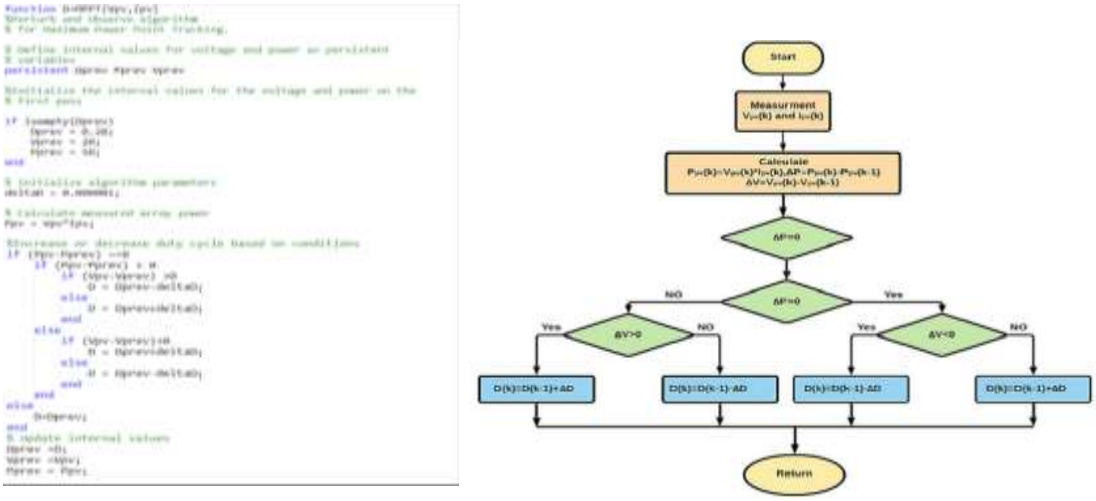

Figure 12. The P&O logic inside MATLAB.

IoT-Based Monitoring System

The Internet of Things (IoT) subsystem was implemented using an ESP32 microcontroller to enable real-time monitoring of photovoltaic (PV) system performance and ambient environmental conditions [52,53]. The ESP32 collects data through an application programming interface (API) connected to the MPPT controller and a weather data service.

The monitored parameters include PV output power, charger voltage and current, battery voltage, ambient temperature, solar irradiance, and cloud cover. These data are periodically transmitted to the Arduino IoT Cloud platform, where they are processed, stored, and visualized via an interactive web-based dashboard.

The dashboard provides real-time visualization of electrical and environmental parameters, as well as power generation trends, enabling continuous system evaluation and diagnostics. The monitoring interface, shown in Figure 13, demonstrates the capability of the proposed IoT framework for effective remote supervision of the PV system.

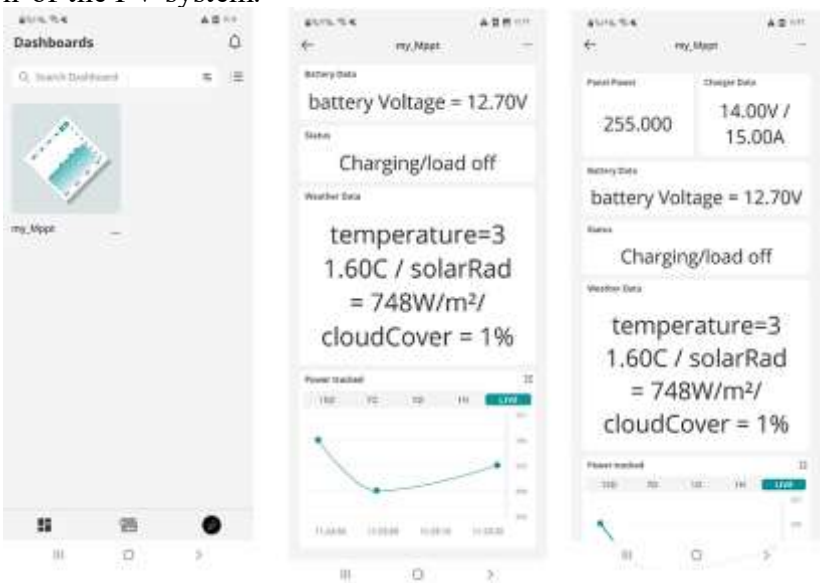

Figure 13. The MPPT monitoring User phone app

Results and Discussion

Figure 14 illustrates the complete photovoltaic (PV) energy conversion system, including the PV array, MPPT controller, Ćuk converter, and Buck converter, implemented in MATLAB/Simulink to evaluate dynamic performance under varying environmental conditions.

The simulation scenarios were conducted using the operating conditions summarized in Tables 1 and 2, derived from the PV characteristics shown in Figures 5–7. These results demonstrate the dependence of output power on variations in solar irradiance at constant temperature (Table 1) and on temperature changes at fixed irradiance (Table 2).

Table 1 presents the PV output power at different irradiance levels under a constant temperature of 25 °C, while Table 2 shows the variation in output power with temperature at a fixed irradiance of 1000 W/m². As expected, the extracted power decreases with reduced irradiance and increased temperature, consistent with the physical behavior of silicon-based PV modules.

Table 1: The power values for different values of irradiance at T=25 °C

Irradiance (W/m^2)	Power (W)
1000	265
800	212.8
500	132.94
400	105.99

Table 2: The power values for different values of T at irradiance =1000W/m^2

Temperature (°C)	Power (W)
25	265.3
30	259.8
45	244

Simulation results confirm that the proposed MPPT-based solar charge controller effectively tracks the maximum power point (MPP) under different operating conditions while maintaining an appropriate voltage level for battery charging. The convergence times for different irradiance and temperature scenarios (highlighted in Tables 1 and 2) are summarized in Table 3.

Table 3: Time (Sec) to reach the MPPT for different values of irradiance and temperature.

Case	Time taken to reach Maximum Power in Sec
1000 w/m^2 and 25 °C	0.054
500 w/m^2 and 25 °C	0.165
1000 w/m^2 and 45 °C	0.048

At an irradiance of 1000 W/m² and a temperature of 25 °C, the system response shown in Figure 15 indicates that the PV module delivers a peak power of 265.3 W, which closely matches the rated maximum power. The MPPT controller successfully tracks this operating point, resulting in an extracted power of approximately 265 W. The Buck converter regulates the battery charging voltage to 14 V with a charging current of 15.5 A.

When the temperature increases to 45 °C, the maximum tracked power decreases to approximately 244 W, as shown in Figure 16. This reduction is attributed to the negative temperature coefficient of PV cells, which leads to a decrease in output voltage and power with increasing temperature. Under these conditions, the controller maintains a tracked power of 244.2 W, while the battery charging voltage and current are 13 V and 14.5 A, respectively.

Under reduced irradiance of 500 W/m², the extracted power decreases to approximately 133 W, as illustrated in Figure 17. The MPPT controller tracks 132 W, while the Buck converter provides a charging voltage of 9.89 V and a current of 10.69 A. These results are consistent with the theoretical relationship between irradiance and PV output power.

In all irradiance and temperature scenarios, the Buck converter duty cycle is adjusted to maintain an acceptable battery charging voltage. The Perturb and Observe (P&O) algorithm effectively modifies the Cuk converter duty cycle to ensure operation near the maximum power point. The converter outputs exhibit smooth voltage and current waveforms with minimal ripple, ensuring stable power transfer to the Buck stage.

Overall, the proposed controller demonstrates high tracking efficiency, fast convergence to the MPP, and strong robustness under environmental variations, as confirmed by the convergence times summarized in Table 3.

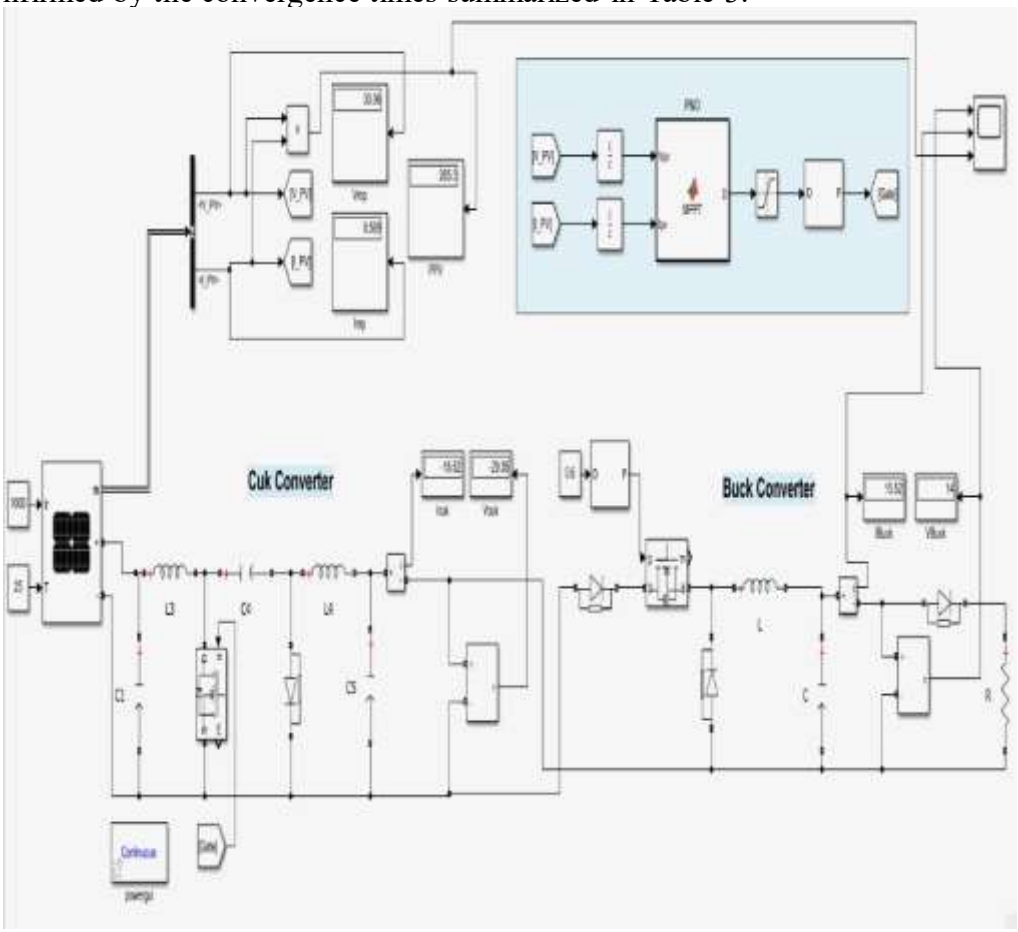

Figure 14. The design PV system with inputs of 1000 w/m² and 25 °C

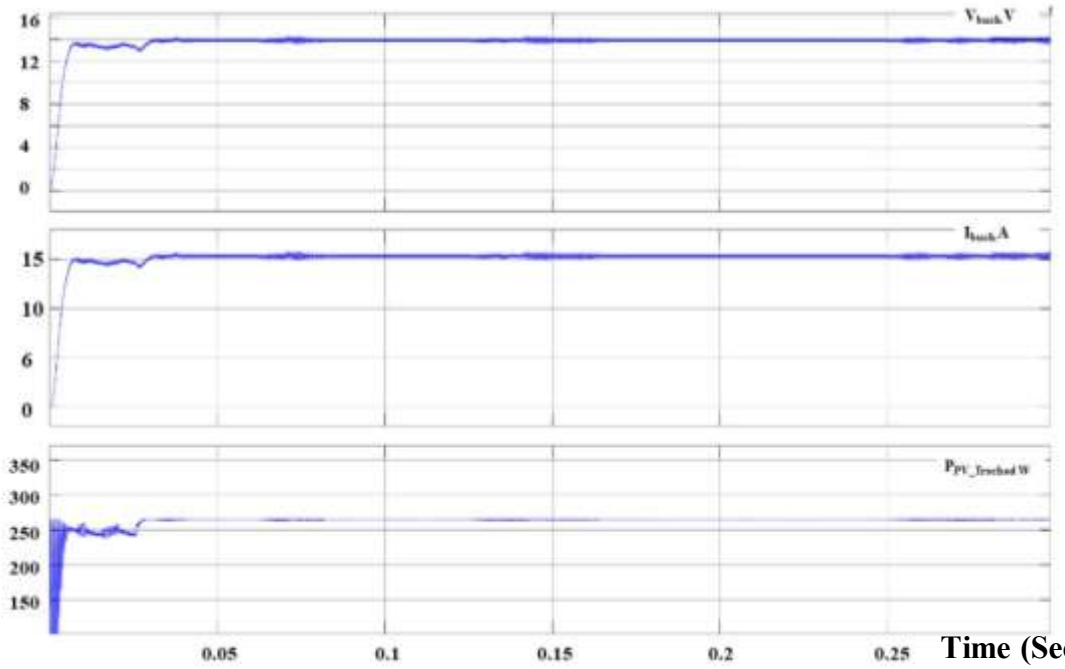

Figure 15.4 Buck converter current, voltage, and tracked PV power under standard test conditions (1000 W/m², 25 °C)

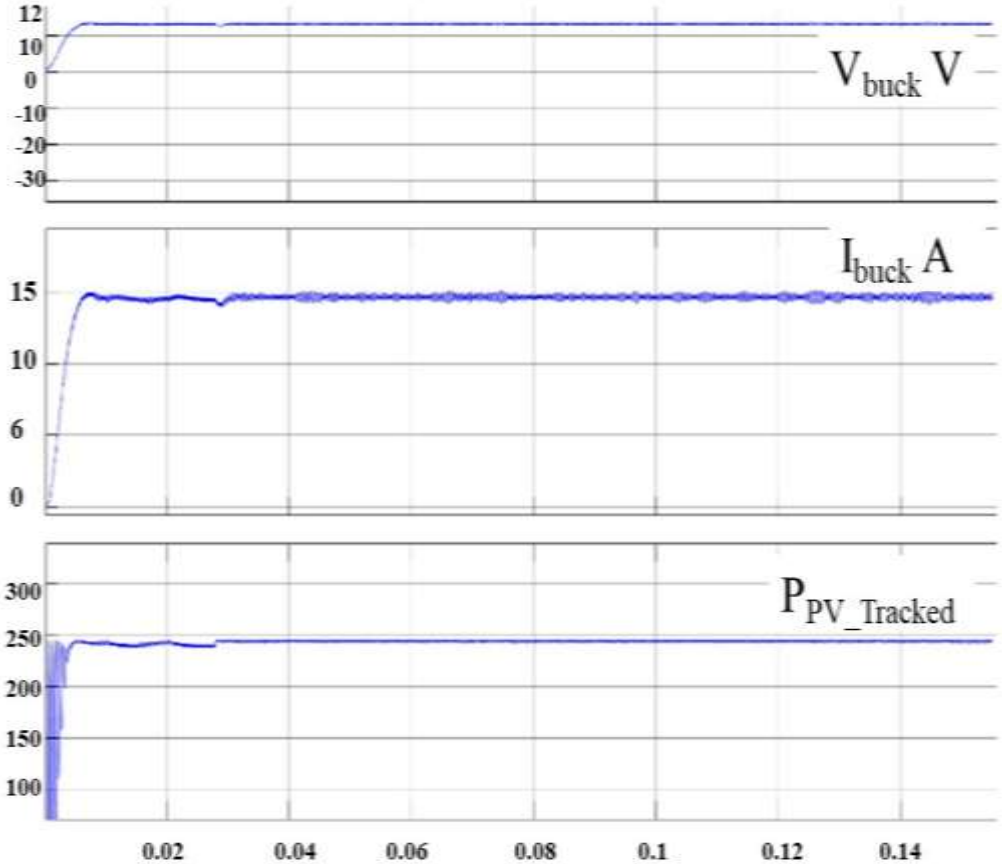

Figure 16. Buck converter current, voltage, and tracked PV power under standard test conditions (1000 W/m², 45 °C)

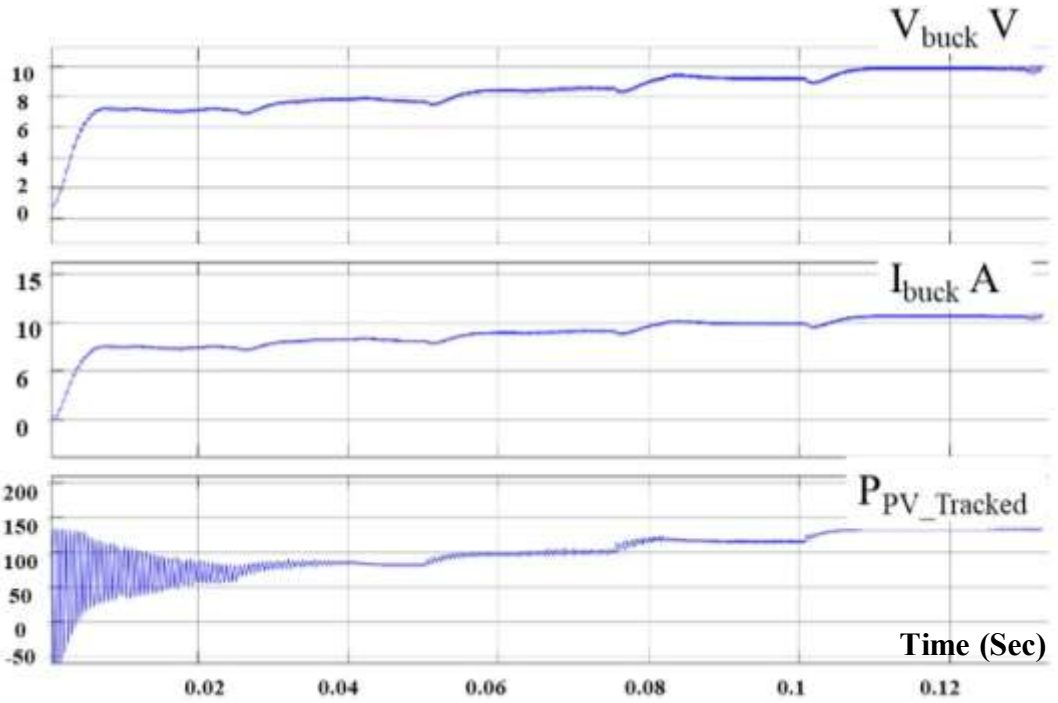

Figure 17. Buck converter current, voltage, and tracked PV power under standard test conditions (500 W/m², 45 °C)

The proposed approach contributes to microgrid systems by improving energy storage management and mitigating associated operational challenges [54-56].

Limitations and Uncertainties

1. Dependence on Environmental Conditions:
   The system performance is highly dependent on solar irradiance and temperature. Severe fluctuations or prolonged low-light conditions can reduce MPPT efficiency and limit total energy harvested.
2. Battery Chemistry Constraints:
   The proposed design is optimized for a 12 V lead-acid battery. Performance and charging stability may vary when applied to other battery chemistries, such as lithium-ion or NiMH, which may require modified charging profiles and voltage regulation strategies.
3. Simulation versus Real-World Implementation:
   Although MATLAB/Simulink results demonstrate fast convergence and high efficiency, practical implementation may introduce deviations due to wiring losses, component tolerances, PV aging effects, and electromagnetic interference.
4. IoT Monitoring Limitations:
   The monitoring system relies on stable internet connectivity. In regions with intermittent network access, real-time data transmission and visualization may be delayed or temporarily unavailable.
5. Converter Non-Idealities:
   The analysis assumes ideal continuous conduction mode operation. In practical systems, switching losses, parasitic resistances, and thermal effects may slightly reduce efficiency and tracking performance.
6. Scalability Constraints:

The proposed architecture is designed for small-scale PV systems. Scaling to larger photovoltaic arrays or higher-voltage battery systems may require redesign of both power stages and control parameters to maintain performance and stability.

Conclusion

This study presents a validated, high-efficiency, and cost-effective dual-stage Maximum Power Point Tracking (MPPT) solar charge controller designed for off-grid photovoltaic applications. The proposed architecture integrates a Perturb and Observe (P&O)-controlled Ćuk converter as the primary MPPT stage with a downstream Buck converter dedicated to battery voltage regulation.

This decoupled configuration effectively separates power extraction from voltage regulation, improving system stability and simplifying control implementation. MATLAB/Simulink simulation results demonstrate a fast dynamic response, with the controller achieving convergence to the maximum power point (MPP) within 0.048–0.165 s under varying irradiance conditions. The system consistently maintained accurate power tracking and efficient energy utilization, confirming the suitability of the Ćuk–Buck topology for photovoltaic charging applications requiring high efficiency and low ripple operation.

Furthermore, the integration of an ESP32-based Internet of Things (IoT) monitoring platform enables real-time data acquisition, remote supervision, and performance analysis. This aligns with current trends in smart energy management for decentralized renewable energy systems [39–40].

Future work will focus on hardware implementation and the development of advanced MPPT techniques, such as incremental conductance and artificial intelligence-based algorithms, to further reduce steady-state oscillations and improve global MPP tracking under partial shading conditions. These enhancements are expected to optimize battery charging profiles, extend battery lifespan, and increase the overall reliability of standalone PV energy systems.

References

1. Fathi, Y., et al. (2025). Technical and environmental cost-benefit analysis of strategies towards a green economy in the electricity sector in Libya. *Economics and Policy of Energy and the Environment*, 2, 133–167.
2. Nassar, F., et al. (2025). Towards green economy: Case of electricity generation sector in Libya. *Solar Energy and Sustainable Development Journal*, 14(1), 334–360.
3. Ahmed, B., et al. (2026). Optimal design of hybrid renewable energy system (PV/Wind/PHS) under multiple constraints of grid connection: A case study. *Wadi Alshatti University Journal of Pure and Applied Sciences*, 4(1), 83–93.
4. Nassar, Y., et al. (2026). Feasibility of concentrating solar power as a solar fuel for electrical power stations: A case study of Ubari Gas-Power Station in Libya. *Wadi Alshatti University Journal of Pure and Applied Sciences*, 4(1), 56–69.
5. Khaleel, M., et al. (2025). Renewable energy transition pathways and net-zero strategies. *International Journal of Electrical Engineering & Sustainability*, 3(4), 1–16.
6. Alkhazmi, A., et al. (2026). Design and analysis of PV solar street lighting systems in remote areas: A case study. *Wadi Alshatti University Journal of Pure and Applied Sciences*, 4(1), 1–14.

7. Al-Jamasi, A., et al. (2022). Social awareness of renewable energy among engineering students. *An-Najah University Journal for Research – B*, 36(6), 1173–1194.
8. El-Batta, F. F., & El-Khozondar, H. J. (2022). Solar energy implementation at household in Gaza Strip. *Energy, Sustainability and Society*, 12, 12–17.
9. El-Batta, F., & El-Khozondar, H. J. (2018). Solar energy as an alternative in Gaza Strip. *An-Najah University Journal for Research – A*, 32(1), 47–74.
10. Imbayah, I., et al. (2026). Modeling a 600 MW floating PV system in Libya. *Wadi Alshatti University Journal*, 4(1), 223–237.
11. Al-Maghalseh, M., et al. (2026). Thermal comfort of BIPV systems. *Wadi Alshatti University Journal*, 4(1), 146–164.
12. Amer, K., et al. (2025). 3E analysis of PV systems. *Wadi Alshatti University Journal*, 3(1), 51–58.
13. Al-Maghalseh, M. (2025). Environmental impact of PV plants. *Wadi Alshatti University Journal*, 3(2), 16–31.
14. Almhdi, E., & Miskeen, G. (2025). Carbon footprint in data centres. *Wadi Alshatti University Journal*, 3(2), 221–229.
15. Amhimmid, A. A., et al. (2024). Wind farm impact in Libya. *International Journal of Energy and Environmental Engineering*, 15(4), 1–20.
16. Albardawil, M., et al. (2025). Solar street lighting in Gaza. *Energy 360*, 4, 100042.
17. Ali, A., et al. (2025). Solar street lighting analysis. *Wadi Alshatti University Journal*, 3(1), 142–150.
18. Alsharif, A. H., et al. (2024). PV street lighting case study. *Power Engineering and Thermophysics*, 3(2), 77–91.
19. El Halim, A., et al. (2023). Off-grid PV system for Gaza Seaport. *IEEE Conference Proceedings*, 10209467.
20. Al-Najjar, H., et al. (2020). Renewable resources analysis. *Designs*, 4(3), 1–8.
21. El-Khozondar, H. J., & El-Batta, F. (2021). Hybrid energy system Gaza. *International Conference on Electric Power Engineering*.
22. Pfeifer, C., et al. (2021). Gaza microgrid system. *SEEP Conference*.
23. Al-Najjar, H., et al. (2022). PV-biogas hybrid system. *Energies*, 15, 3151.
24. Al Afif, R., et al. (2019). Renewable energy lab implementation. *IEEE ICPCEC*.
25. Pfeifer, C., et al. (2019). Solar-powered toilet system. *IEEE ICPCEC*.
26. El-Khozondar, H. J., et al. (2023). Hybrid PV/wind/diesel system. *Environmental Progress & Sustainable Energy*, 42(3), e14049.
27. Aqila, A., et al. (2025). Hybrid PV system Libya. *Wadi Alshatti University Journal*, 3(1), 168–181.
28. Salim, E., et al. (2025). Pumped hydro storage system. *Wadi Alshatti University Journal*, 3(1), 152–167.
29. Abduallah, A., et al. (2025). Grid storage integration. *Wadi Alshatti University Journal*, 3(2), 322–332.
30. El-Batta, F., et al. (2021). Hybrid energy system design. *SSRN*, 3880850.
31. El-Batta, F. F., & El-Khozondar, H. J. (2018). Solar usage survey. *IOP Conference Series*, 1108, 012125.
32. Matter, K., et al. (2015). PV modeling under shading. *International Research Journal of Engineering and Technology*, 2(2), 697–703.

33. Matter, K., et al. (2015). PV parameter analysis. *Energy Procedia*, 74, 1142–1149.
34. Osmani, K., et al. (2023). MPPT battery charger. *Sustainability*, 15(12), 9839.
35. Suntio, T., et al. (2016). MPPT algorithms review. *Renewables*, 3(3), 1–8.
36. El-Khozondar, H. J., & Matter, K. (2015). Incremental conductance MPPT. *Journal of Mechatronics*, 3(2), 174–178.
37. Matter, K., et al. (2014). MPPT comparison. *International Conference on Engineering Sustainability*, 372–379.
38. Koch, A. W., et al. (2019). MPPT comparative study. *IEEE ICPCEC*.
39. Kaaitan, M. T., et al. (2025). Global MPPT optimization. *Scientific Reports*.
40. Alkarasneh, A., et al. (2024). Fuzzy MPPT algorithm. *Jordan Journal of Mechanical and Industrial Engineering*, 18(4).
41. Al-Mathnani, A., et al. (2025). PV control system. *Wadi Alshatti University Journal*, 3(1), 30–34.
42. Hadi, S. M. (2025). Adaptive MPPT method. *University of Babylon Engineering Journal*, 33(3).
43. Abuqila, M., et al. (2025). Battery storage estimation. *Wadi Alshatti University Journal*, 3(1), 58–71.
44. Awad, M., et al. (2022). PV EV charging system. *Frontiers in Energy Research*, 10, 969482.
45. Dalla, L., et al. (2026). IoT PV fault detection. *Wadi Alshatti University Journal*, 4(1), 41–55.
46. Sahmoud, A., et al. (2025). PV cell performance. *Solar Energy*, 291, 113410.
47. Pfeifer, C., et al. (2021). Solar cell coating. *International Journal of Thermofluids*, 11, 100103.
48. Assidiq, A. R., et al. (2024). Ćuk converter topology. *e-Prime*, 9, 100654.
49. Albuzia, D., et al. (2025). Boost converter PV system. *Wadi Alshatti University Journal*, 3(2), 192–201.
50. Koch, A. W., et al. (2019). Switching mechanism hybrid system. *IEEE ICPCEC*.
51. Jim, T. W. Y., et al. (2019). PV inverter simulation. *IEEE ICPCEC*.
52. Bayoumi, E., et al. (2024). IoT energy monitoring system. *e-Prime*, 6(2), 129–137.
53. Imbayah, I., et al. (2024). Smart farms IoT Libya. *Sebha University Conference*, 3(2).
54. Khaleel, M., et al. (2024). Smart grid technologies. *International Journal of Electrical Engineering & Sustainability*, 2(2), 62–82.
55. El-Khozondar, H. J., et al. (2025). Hybrid renewable system assessment Gaza. *Engineering Science and Technology, an International Journal*, 69, 102120.
56. Diaz, P., & El-Khozondar, H. (2019). Energy storage technologies review. *IEEE ICPCEC*.